

Nanoprecipitation Based Preparation and Physicochemical Characterization of Flavonoid Nanoparticles

Kiran Prabhakar Sinkar, Piyush Shantilal Bafna & Rakesh Eshwarlal Mutha*

Department of Pharmacognosy, H. R. Patel Institute of Pharmaceutical Education and Research,
Shirpur, Dist. Dhule, Maharashtra, India

*Email: rakeshmutha123@yahoo.co.in

Abstract

Out of different secondary metabolites, flavonoids attract the attention of researchers due to their pharmacological potential and health benefits. But solubility and bioavailability issues severely restrict their use. Development of nanoformulation of flavonoids is one of the solutions to overcome these issues. The purpose of this study was to develop and characterize chrysin (CHR) loaded nanoparticles (CHRN) by nanoprecipitation technique with Eudragit® and polyvinyl alcohol (PVA) as carriers. Particle size, polydispersity index (PDI), zeta potential, scanning electron microscopy (SEM), Fourier-transform infrared spectroscopy (FTIR) and X-ray powder diffraction (XRPD) was used to characterize the prepared CHRN. The present study shows that CHRN can be fabricated by a nanoprecipitation technique using the optimum weight ratio of CHR: Eudragit: PVA (1: 5: 5). The particle size, PDI, and zeta potential were found to be 238.1 nm, 0.434 and -20.1 mV. According to FTIR, CHR developed intermolecular hydrogen bonds with polymers (carriers). SEM imaging confirmed roughly spherical type particles with size of 100–400 nm. The results from the XRPD of the CHRN showed that the crystal of the drug might be converted to an amorphous state. The release of the drug from the CHRN was 85.54% compared with the pure drug at 45.11%.

Keywords: Chrysin, Carrier, Nanoparticles, Nanoprecipitation technique, Polymer

Introduction

Since the beginning of time, natural remedies have been used to treat a variety of health conditions. One of the important types of secondary metabolites is polyphenolics. It consists of around 8000 polyphenolic molecules that are found in various plants. The subclasses of polyphenolic substances include phenolic alcohols, stilbenoids, flavonoids, phenolic acids and lignans. Flavonoids have been recognized as one of the most significant and prevalent classes of all plant phenolics among these substances. This is due to their biological and pharmacological functions and the therapeutic effects on health (Gattuso et al., 2007).

A natural flavonoid called chrysin (5,7-dihydroxyflavone) is derived from plants, propolis, and honey (Mutha & Surana, 2018; Mutha et al., 2021). Numerous studies on chrysin (CHR) have shown that it has a wide variety of pharmacological and biological qualities, including effects that are protective, anti-allergic, antioxidant, anti-

inflammatory and anti-cancer (Anand et al., 2011; Ciftci & Ozdemir, 2011; Khan et al., 2012; Lim et al., 2011; Yang et al., 2013). CHR is of great interest for therapeutic research as well as health food supplements because of its abundance in plants, significant health benefits, nutritional benefits as well as low systemic toxicity. CHR's limited water solubility, which significantly reduces its bioavailability, frequently restricts its use as a drug. It has been recommended that encapsulation into appropriate delivery vehicles can be used to alleviate this issue (Zhu et al., 2016).

There has been significant scientific attention to the use of nanoparticle-based drug delivery systems as carriers for numerous big and small compounds during the past few decades (Nayak & Dhara, 2010; Pal & Nayak, 2010). In general, solid particles with a size between 1 to 100 nm are known as nanoparticles. Due to their stability and accessibility in surface modification, polymeric nanoparticles have gained the most attention among the numerous types of nanoparticles (Liu et al., 2008).

Treatment regimens have been completely transformed by nanocarrier's capacity to direct medications to specific locations in the body. With this, it improves their therapeutic index, increases their solubility and prolongs their half-life. Polymeric nanoparticles are the most adaptable type of nanocarriers. This is because of their adjustable structure which allows them to customize their properties for different purposes (Bertrand et al., 2014; Petros & DeSimone, 2010; Sunoqrot & Abujamous, 2019).

The solvent displacement method commonly referred to as the nanoprecipitation method is the most basic technique for creating polymeric nanoparticles carrying drugs. Fessi and co-workers created and patented this technique initially (Fessi et al., 1989).

The development and characterization of CHR-loaded polymeric nanoparticles were the goals of this investigation. Polyvinyl alcohol (PVA) and eudragit were utilized in the nanoprecipitation method to produce CHR-loaded polymeric nanoparticles. It was anticipated that this approach would increase the drug's rate of dissolving and hence increase its oral bioavailability. These nanoparticles were characterized by particle size, zeta potential, scanning electron microscopy (SEM), fourier transforms infrared spectroscopy (FTIR), X-ray

powder diffraction (XRPD), encapsulation efficiency and *in-vitro* dissolution.

Materials and Methods

Materials

PVA, eudragit, acetone and CHR were purchased from Sigma-Aldrich. All chemicals used were of analytical grade. Deionized water was used throughout this study.

Method of preparation

The weight ratio used in the formulation for CHR: Eudragit: PVA was 1:5:5, i.e., 50 mg: 250 mg: 250 mg. In 25 mL of acetone CHR and eudragit were dissolved (Internal organic phase). PVA was dissolved in 75 mL of distilled water (external aqueous phase). In the external aqueous phase, internal organic phase was quickly injected with continuous stirring at 1000 rpm and then ultrasonicated using probe sonication (PCI Analytics, India). Rotary vacuum evaporation (SAM-REV-0.25, Spire automation, India) was used to remove acetone. After that, a freeze dryer (Southern scientific lab instrument, India) was used for lyophilization of the remaining fraction. The lyophilized powder was collected and stored in an air-tight container (Kumar et al., 2020; Wu et al., 2008).

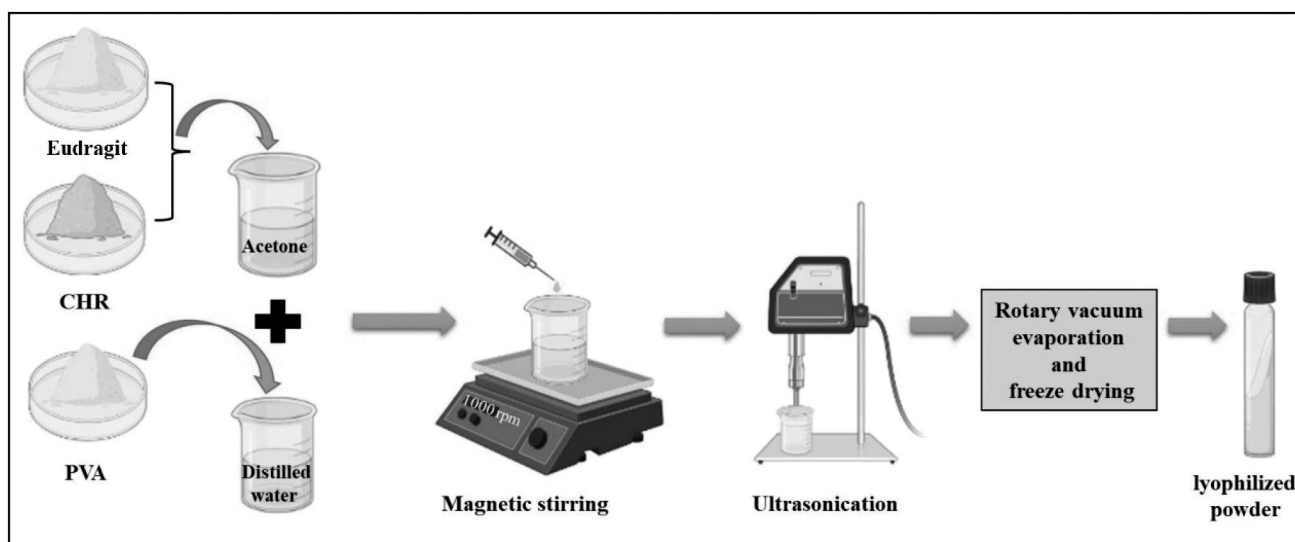


Figure 1: Method of preparation of CHR-loaded nanoparticles (CHRNs)

Particle size, zeta potential, and polydispersity index (PDI)

Particle size, PDI and zeta potential were determined with the help of Malvern Zetasizer Nano-ZS, UK. DLS techniques were used to measure the size of the particles. By using Laser-Doppler-microelectrophoresis, the surface charge (zeta potential) of the nanoparticles was determined. For the purpose of determining the CHRNs' particle size and zeta potential, it was diluted in deionized water (Awet et al., 2018).

Fourier transform infrared spectroscopy

Using an FTIR spectrometer (IR Affinity, Shimadzu), FTIR spectra of pure CHR powder, eudragit, PVA, and freeze dried CHRNs were obtained. Each sample was combined at 1:100 with IR grade potassium bromide before being placed directly on the pan for the FTIR analysis. The FTIR analysis was done in a scanning range of 4000 cm⁻¹ to 400 cm⁻¹ (Jiang et al., 2019; Tade et al., 2018).

X-ray powder diffraction

X-ray diffraction utilizing a Bruker D8 advance diffractometer with CuK α ($\lambda=1.5406\text{\AA}$) radiation was used to characterize the powders (Bruker AXS, D8 Advance). Dry samples (CHR powder, eudragit, PVA and CHRNs) were recorded in the scattering range of 2 θ (0°-60°) at a 151 speed of 2°/min at room temperature (Bi et al., 2016; Wu et al., 2019).

Scanning electron microscopy

The produced nanoparticle's structural morphology was investigated using SEM. An SEM, Jeol JSM-5800 LV model, Japan, with an accelerating voltage of 15 kV, was used to image the produced nanoparticles after they had been sputter coated with gold using SPI 11430 sputter coater (Naik et al., 2016; Zhong & Yun, 2015).

Entrapment efficiency (EE)

Centrifugation was used to measure CHR entrapment efficiency in the produced nanosuspension. The untrapped CHR was removed from the nanosuspension using centrifugation (Etek Overseas

Pvt. Ltd., India) at 10000 rpm for 30 minutes (Salatin et al., 2017; Patil & Dhawale, 2018).

$$\% \text{ EE} = \frac{\text{Actual drug content in nanoparticles}}{\text{Total drug used in formulation}} \times 100$$

In-vitro drug release study

The developed nanoparticles *in-vitro* drug release was assessed using the dialysis bag (DB) diffusion method. Before the experimental procedure started, the DB (Himedia, Mol. Wt. cut-off 12000 Da) was previously soaked in pH 1.2 HCl buffer for 24 hrs. The *in-vitro* release of CHR (50 mg) and CHRNs (50 mg CHR equivalent) was assessed using the diffusion technique and a dissolution instrument (Dissolution test TDT-08Lx, Electrolab, India). After putting CHRNs and CHR into the DB and soaking it in 900 mL of pH 1.2 HCl buffer for two hours, the experiment was started. As part of an ongoing study, dialysis bags were transferred to a pH 7.4 phosphate buffer. Maintained condition at 37 \pm 1°C with a speed of 100 rpm. At regular time intervals, 5 mL aliquots were collected. The sink condition was maintained by using the same volume of fresh dissolving medium and was then added to the dissolution container. At first, the aliquots were filtered, appropriately diluted and finally, absorbance was measured at a wavelength of 268 nm with a UV-vis spectrophotometer (Deshmukh et al., 2021; Gandhi et al., 2014).

Results and Discussion

Particle size, zeta potential and PDI

The performance of the nanocarrier is significantly influenced by its size and surface charge. DLS was used to examine particle size and surface charge (Sunoqrot & Abujamous, 2019). The most important factor for the effective application of this kind of formulation is particle size. Particle size and dispersion were significantly affected by the contents of the polymer and the surfactant (Patil & Dhawale, 2018). The average particle diameter (Figure 2) of the synthesized CHRNs and zeta potential (Figure 3) were found to be 238.1 nm and -20.1 mV, respectively. The polydispersity values (Figure 2) for synthesized CHRNs were found to be 0.434.

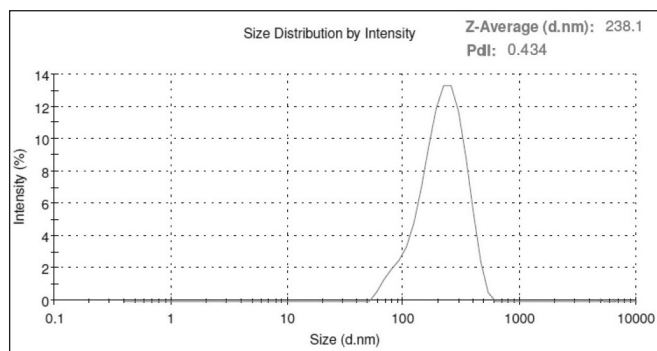


Figure 2: Particle size and PDI of CHRNs

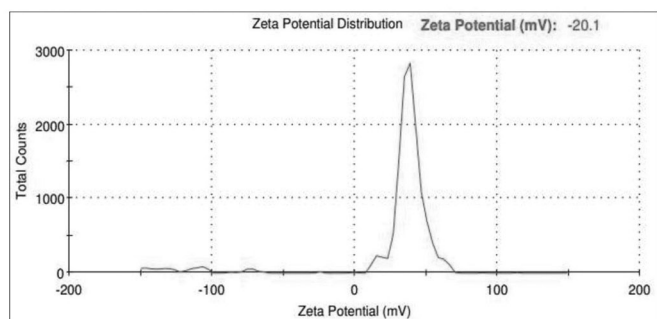


Figure 3: Zeta potential of CHRNs

Fourier transform infrared spectroscopy

The interaction between the drug and polymers were examined using FTIR analysis of samples. Figure 4 indicates the FTIR peaks of pure CHR, Eudragit, PVA, and CHRNs. In CHRNs, the intensity and broadening of O-H peaks have decreased. This may be due to the interactions between CHR and polymers via intermolecular H-bonds (Sunqrot & Abujamous, 2019). As per the obtained FTIR spectrum of CHRNs, the IR absorption in the range

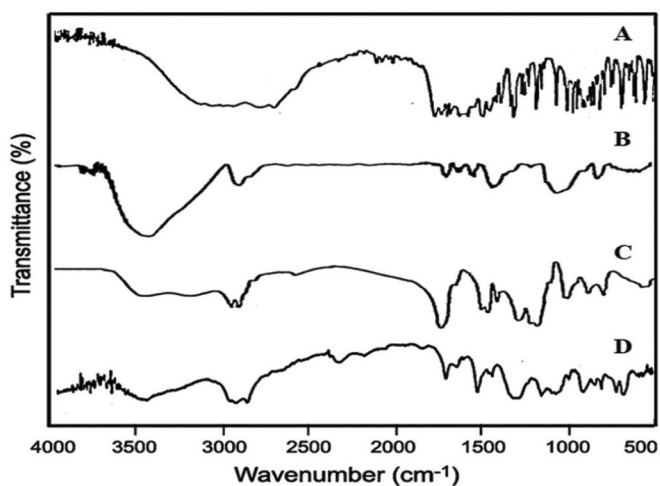


Figure 4: FTIR spectra of, A. CHR, B. PVA, C. Eudragit, D. CHRNs

1639, 1248 indicates the presence of C=C stretch and C-O stretch respectively, which confirms that the functional group of CHR was unchanged in the spectrum of CHRNs. CHRNs spectrum closely matches the spectrum of CHR and polymers which indicates that there isn't any chemical interaction among the precursors. Furthermore, the preparation method was suitable to prepare CHRNs as retention of peaks of CHR in CHRNs were observed.

X-ray powder diffraction

The physical characteristics of the drug that was encapsulated were examined using the powder XRD diffraction method. Diffraction patterns obtained for PVA, Eudragit, CHR and CHRNs are presented in Figure 5. The powder XRD of PVA and eudragit confirmed their amorphous nature. The powder XRD of CHR shows highly crystalline in nature. All the crystalline peaks of CHR were masked by the polymers due to encapsulation of CHR in polymers. Due to this, the diffraction pattern of CHRNs resembled that of PVA (Sunqrot & Abujamous, 2019).

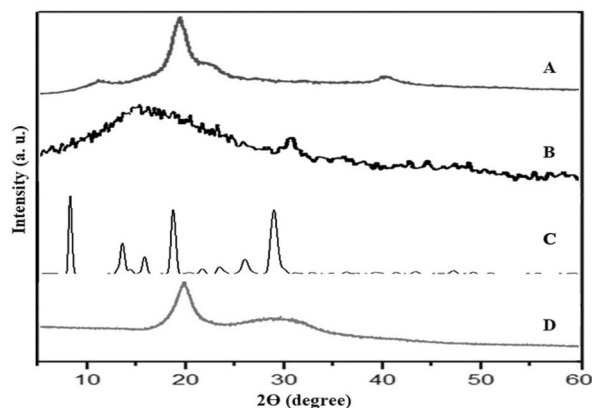


Figure 5: XRPD patterns of, A. PVA, B. Eudragit, C. CHR, D. CHRNs

Scanning electron microscopy

Images captured by scanning electron microscopy show how CHRNs and pure drugs surfaces differ (Figure 6). The surface morphology of the pure CHR (A) showed irregular shape but nanoparticles (B) are roughly spherical in shape and particle size varies in 100-400 nm range. It was also observed that the majority of nanoparticles were between 100 and 300 nm in diameter.

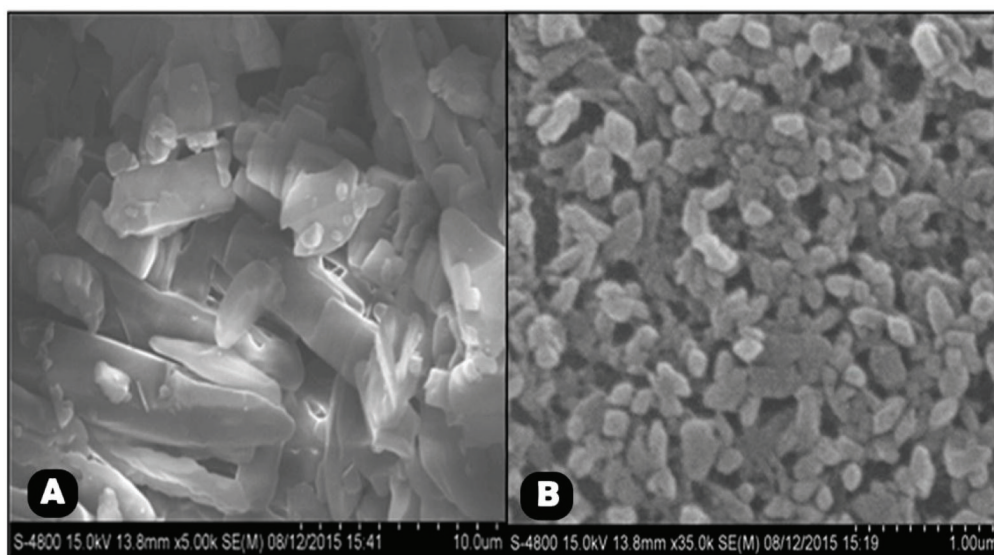


Figure 6: SEM images of, **A.** pure CHR at 10µm scale, **B.** CHRNs at 1µm scale

Entrapment efficiency

Drug entrapment efficiency was expressed as the percentage of CHR entrapped in these prepared polymeric nanoparticles and the drug: polymer (CHR: Eudragit: PVA) ratio was 1: 5: 5. The entrapment efficiency of polymeric nanoparticles was found to be 88.74%.

In-vitro drug release study

Using the dialysis bag diffusion method in phosphate buffer, pH 1.2 and 7.4, the *in-vitro* drug release from the synthesized CHR loaded nanoparticles and pure CHR was assessed. Over the course of 24 hrs., it was observed that these nanoparticles sustained the cumulative percentage of CHR release (% CDR) (Figure 7). This study discovered that the pure CHR released from drug suspension after 24 hrs. was only 45.11 %, as opposed to CHRNs at 85.54 % (Figure 7). Higher wettability and solubility may result in enhanced release of CHR from the CHRNs due to the amorphous form of entrapped CHR in comparison to pure CHR. The CHRNs improved dissolution profile might be the result of significant drug entrapment. CHR separates from the polymer-drug combination in an aqueous media as CHR is released from CHRNs in a continuous way. As a result, CHRNs increase the rate and extent of CHR release in comparison to pure CHR (Deshmukh et al., 2021).

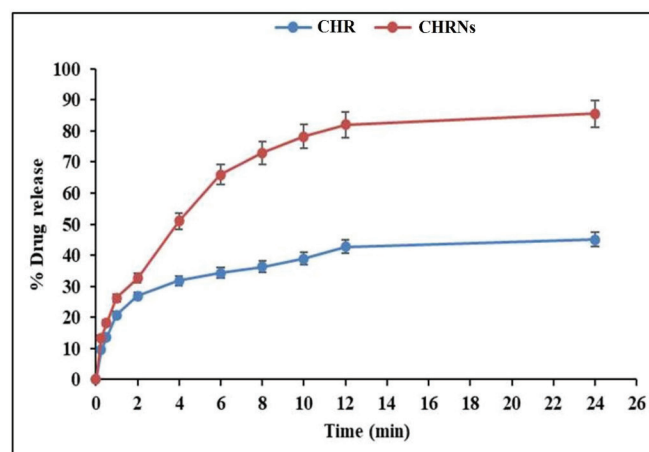


Figure 7: *In-vitro* drug release study of pure CHR and CHRNs

Conclusion

In this study, CHR loaded polymeric nanoparticles were prepared by using the nanoprecipitation technique. An optimized formulation composition ratio was (CHR: Eudragit: PVA) 1: 5: 5. The average particle size, polydispersity index and zeta potential were found to be 238.1 nm, 0.434, and -20.1 mV respectively. The FTIR analysis indicated the formation of intermolecular H-bonding between CHR and the polymers. XRD analysis also revealed that CHR was present in the nanoparticles in an amorphous state. The surface morphology of CHR was irregular, after encapsulation of CHR nanoparticles, surface morphology changed

to roughly spherical in shape. The entrapment efficiency of CHR was found to be 88.74%. *In-vitro* release of CHR loaded polymeric nanoparticles confirmed increased aqueous solubility and bioavailability of CHR. The drug release of CHR loaded polymeric nanoparticles after 24 hrs. was found to be 85.54% and pure drug released only 45.11%. This study should be extended further in *in vivo* and pharmacology studies of prepared nanoparticles to ascertain its use as an anticancer drug in near future.

Author Contributions

All the authors were involved in concept development, research designing, defining intellectual content and literature research. K. Sinkar collected and analyzed data and prepared the manuscript. P. Bafna and R. Mutha edited and reviewed the manuscript. R. Mutha as a corresponding author, is the guarantor for this article.

Acknowledgments

The authors would like to thank Dr. S. B. Bari, Principal H. R. Patel Institute of Pharmaceutical Education and Research, Shirpur for availing all the necessary requirements to carry out this research work.

References

- Anand, K. V., Anandhi, R., Pakkiyaraj, M., & Geraldine, P. (2011). Protective effect of chrysin on carbon tetrachloride (CCl₄)-induced tissue injury in male Wistar rats. *Toxicology and Industrial Health*, 27(10), 923-933.
- Awet, T. T., Kohl, Y., Meier, F., Straskraba, S., Grün, A. L., Ruf, T., Jost, C., Drexel, R., Tunc, E., & Emmerling, C. (2018). Effects of polystyrene nanoparticles on the microbiota and functional diversity of enzymes in soil. *Environmental Sciences Europe*, 30(1).
- Bertrand, N., Wu, J., Xu, X., Kamaly, N., & Farokhzad, O. C. (2014). Cancer nanotechnology: the impact of passive and active targeting in the era of modern cancer biology. *Advanced Drug Delivery Reviews*, 66, 2-25.
- Bi, Y., Wang, T., Liu, M., Du, R., Yang, W., Liu, Z., Peng, Z., Liu, Y., Wang, D., & Sun, X. (2016). Stability of Li₂CO₃ in cathode of lithium ion battery and its influence on electrochemical performance. *RSC Advances*, 6(23), 19233-19237.
- Ciftci, O., & Ozdemir, I. (2011). Protective effects of quercetin and chrysin against 2,3,7,8-tetrachlorodibenzo-p-dioxin (TCDD) induced oxidative stress, body wasting and altered cytokine productions in rats. *Immunopharmacology and Immunotoxicology*, 33(3), 504-508.
- Deshmukh, P. K., Mutha, R. E., & Surana, S. J. (2021). Electrostatic deposition assisted preparation, characterization and evaluation of chrysin liposomes for breast cancer treatment. *Drug Development and Industrial Pharmacy*, 47(5), 809-819.
- Fessi, H., Puisieux, F., Devissaguet, J. P., Ammoury, N., & Benita, S. (1989). Nanocapsule formation by interfacial polymer deposition following solvent displacement. *International Journal of Pharmaceutics*, 55(1), R1-R4.
- Gandhi, A., Jana, S., & Sen, K. K. (2014). In-vitro release of acyclovir loaded Eudragit RLPO® nanoparticles for sustained drug delivery. *International Journal of Biological Macromolecules*, 67, 478-482.
- Gattuso, G., Barreca, D., Gargiulli, C., Leuzzi, U., & Caristi, C. (2007). Flavonoid composition of citrus juices. *Molecules*, 12(8), 1641-1673.
- Jiang, L., Yang, J., Wang, Q., Ren, L., & Zhou, J. (2019). Physicochemical properties of catechin/ β -cyclodextrin inclusion complex obtained via co-precipitation. *CyTA-Journal of Food*, 17(1), 544-551.
- Khan, R., Khan, A. Q., Qamar, W., Lateef, A., Tahir, M., Rehman, M. U., Ali, F., & Sultana, S. (2012). Chrysin protects against cisplatin-induced colon toxicity via amelioration of oxidative stress and apoptosis: Probable role of p38MAPK and p53. *Toxicology and Applied Pharmacology*, 258(3), 315-329.

- Kumar, N., Aggarwal, R., & Chauhan, M. K. (2020). Extended levobunolol release from Eudragit nanoparticle-laden contact lenses for glaucoma therapy. *Future Journal of Pharmaceutical Sciences*, 6(1).
- Lim, H., Jin, J. H., Park, H., & Kim, H. P. (2011). New synthetic anti-inflammatory chrysin analog, 5,7-dihydroxy-8-(pyridine-4yl) flavone. *European Journal of Pharmacology*, 670(2-3), 617-622.
- Liu, Z., Jiao, Y., Wang, Y., Zhou, C., & Zhang, Z. (2008). Polysaccharides-based nanoparticles as drug delivery systems. *Advanced Drug Delivery Reviews*, 60(15), 1650-1662.
- Mutha, R. E., & Surana, S. J. (2018). Ultrasonic frequency based development of chrysin nanoparticles: Assessment of bioavailability, anti-cancer activity and stability. *Materials Technology*, 33(7), 495-505.
- Mutha, R. E., Tatiya, A. U., & Surana, S. J. (2021). Flavonoids as natural phenolic compounds and their role in therapeutics: An overview. *Future Journal of Pharmaceutical Sciences*, 7(1).
- Naik, K., Chandran, V. G., Rajashekar, R., Waigaonkar, S., & Kowshik, M. (2016). Mechanical properties, biological behaviour and drug release capability of nano TiO₂-HAp-Alginate composite scaffolds for potential application as bone implant material. *Journal of Biomaterials Applications*, 31(3), 387-399.
- Nayak, A. K., & Dhara, A. K. (2010). Nanotechnology in drug delivery applications: A review. *Archives of Applied Science Research*, 2(2), 284-293.
- Pal, D., & Nayak, A. K. (2010). Nanotechnology for targeted delivery in cancer therapeutics. *International Journal of Pharmaceutical Sciences Review and Research*, 1(1), 1-7.
- Patil, P. S., & Dhawale, S. C. (2018). Development of ritonavir loaded nanoparticles: In-vitro and in vivo characterization. *Asian Journal of Pharmaceutical and Clinical Research*, 11(3), 284.
- Petros, R. A., & DeSimone, J. M. (2010). Strategies in the design of nanoparticles for therapeutic applications. *Nature Reviews Drug discovery*, 9(8), 615-627.
- Salatin, S., Barar, J., Barzegar-Jalali, M., Adibkia, K., Kiafar, F., & Jelvehgari, M. (2017). Development of a nanoprecipitation method for the entrapment of a very water soluble drug into Eudragit RL nanoparticles. *Research in Pharmaceutical Sciences*, 12(1), 1.
- Sunogrot, S., & Abujamous, L. (2019). pH-sensitive polymeric nanoparticles of quercetin as a potential colon cancer-targeted nanomedicine. *Journal of Drug Delivery Science and Technology*, 52, 670-676.
- Tade, R. S., More, M. P., Chatap, V. K., Patil, P. O., & Deshmukh, P. K. (2018). Fabrication and In-vitro drug release characteristics of magnetic nanocellulose fiber composites for efficient delivery of nystatin. *Materials Research Express*, 5(11), 116102.
- Wu, C., Sun, J., Chen, M., Ge, Y., Ma, J., Hu, Y., Pang, J., & Yan, Z. (2019). Effect of oxidized chitin nanocrystals and curcumin into chitosan films for seafood freshness monitoring. *Food Hydrocolloids*, 95, 308-317.
- Wu, T. H., Yen, F. L., Lin, L. T., Tsai, T. R., Lin, C. C., & Cham, T. M. (2008). Preparation, physicochemical characterization, and antioxidant effects of quercetin nanoparticles. *International Journal of Pharmaceutics*, 346(1-2), 160-168.
- Yang, F., Jin, H., Pi, J., Jiang, J. H., Liu, L., Bai, H. H., Yang, P. H., & Cai, J. Y. (2013). Antitumor activity evaluation of novel chrysin-organogermanium (IV) complex in MCF-7 cells. *Bioorganic Medicinal Chemistry Letters*, 23(20), 5544-5551.
- Zhong, L., & Yun, K. (2015). Graphene oxide-modified ZnO particles: synthesis, characterization, and antibacterial properties. *International Journal of Nanomedicine*, 10(Spec Iss), 79-92.
- Zhu, Z. Y., Luo, Y., Liu, Y., Wang, X. T., Liu, F., Guo, M. Z., Wang, Z., Liu, A. J., & Zhang, Y. M. (2016). Inclusion of chrysin in β -cyclodextrin and its biological activities. *Journal of Drug Delivery Science and Technology*, 31, 176-186.